Reply to referee comments

On heating of solar wind protons by the breaking of large amplitude Alfvén waves

Manuscript ID: angeo-2018-14 (AngeoComm)
H. Comişel, Y. Nariyuki, Y. Narita, and U. Motschmann

5   Thank you very much for reading the manuscript and raising helpful comments and suggestions.

– *This manuscript describes a hybrid kinetic simulation study of a parametric instability in which two counter-propagating Alfven waves couple with a spectrum of ion acoustic modes to transfer fluctuation energy from the former into the latter. This is an interesting configuration to examine, but the manuscript is incomplete because it does not clearly discuss the physical*
10   *consequences of the computation.*

The central problem here is that Figure 3 and the associated discussion is not clearly defined. I do not agree that Figure 3 shows that the velocity distributions are "different for the three analyzed systems"; to my eye the six panels of Figure 3 are qualitatively all the same.

Reply:
15

Figure 3 has been updated by including a missing term ($1/v_\perp$) used to properly compute the velocity distribution function in cylindrical coordinates. The velocity distribution function f is computed by counting the number of particles $dN = f(v_\perp, v_\parallel, \Phi)dV$ in the volume element $dV = v_\perp dv_\perp dv_\parallel d\Phi$, and by integrating over the azimuthal Φ angle. Here, $v_\perp = \sqrt{v_{\perp 1}^2 + v_{\perp 2}^2}$
20   is the velocity component perpendicular to the mean magnetic field, $v_\parallel$ is the parallel velocity, and the angle $\Phi = \arctan v_{\perp 1}/v_{\perp 2}$ gives the sign of $v_\perp$. At times ($t\Omega_p$=300; $t\Omega_p$=600), the updated plots are slightly different from those shown in former Fig. 3.

We accept the referee criticism that there are no obvious differences between the velocity distributions shown in Fig. 3 (or in new Fig.3). However, one can notice a distinct trend
25   of evolution for the distributions between the intermediate ($t\Omega_p$=300) and the final time of simulation ($t\Omega_p$=600). At the final time, the contour levels in the 3D simulation are moderately enlarging both in the parallel and perpendicular directions by following the contour levels of energy conservation driven by the pitch-angle scattering of protons. The contour levels in 1D and 2D runs, in contrast, are developing mainly towards parallel direction while their initial
30   perpendicular displacement is removing with time elapsing.

Changes in the manuscript:

– Page 5: Line 6 to Line 10:
"The velocity distribution function f is computed by counting the number of parti-
35   cles $dN = f(v_\perp, v_\parallel, \Phi)dV$ in the volume element $dV = v_\perp dv_\perp dv_\parallel d\Phi$, and by integrating over the azimuthal Φ angle. Here, $v_\perp = \sqrt{v_{\perp 1}^2 + v_{\perp 2}^2}$ is the velocity component perpendicular to the mean magnetic field, $v_\parallel$ is the parallel velocity, and the angle $\Phi = \arctan v_{\perp 1}/v_{\perp 2}$ gives the sign of $v_\perp$."
– Page 5: Line 11 to Line 14:
40   "Due to the transversal wave field imposed at the initial condition, the velocity distribution functions are rigid shifted towards the initial bulk velocity $\pm u_\perp$, see e.g., Verscharen2011, Nariyuki2011. The two symmetrical sets of contour levels with respect to

the $v_\perp = 0$ axis are slowly merging with the time evolution and at time tΩ_p=300 there are no remnants of the rigid displacement observed at the initial time."

45   – Former manuscript, Page 5: Line 1 to Line 3 - deleted.

    – Page 6: Line 6 to Line 11:
"Although there are no obvious differences between the velocity distributions in the three different setups, one can notice a distinct trend of evolution for the distributions between 50   the intermediate ($t\Omega_p$=300) and the final time of simulation ($t\Omega_p$=600). At the final time, the contour levels in the 3D simulation are moderately enlarging both in the parallel and perpendicular directions by following the contour levels of energy conservation driven by the pitch-angle scattering of protons. The contour levels in 1D and 2D runs, in contrast, are developing mainly towards parallel direction while their initial perpendicular 55   displacement is removing with time elapsing."

– *I disagree that the final distribution functions for the 3D system ... report a larger perpendicular acceleration. To substantiate this claim, the authors should do the velocity integrations to compute $T_{||}$ and $T_\perp$ as functions of time through the simulation.*

Reply:
60 The time evolutions of $T_{||}$ and $T_\perp$ determined during the simulation runs are shown in new Figure 4. Figure 4 reports that the perpendicular temperature (normalized to its initial value) achieved in the 3D system at the final time ($t\Omega_p$=600) is about two times larger than that one from the 2D system.

Changes in the manuscript:
65

    – Page 6: Line 11 to Line 14:
"The more efficient heating of plasma in the 3D system is consistent with the time evolution of the ion temperature shown in Fig. 4. The particles experience a similar parallel heating while the perpendicular temperature achieved in the 3D system (solid line) dom-70   inates by a factor of two or more the corresponding values obtained in the 1D (dotted line) and 2D (dashed line) simulations. "

– *The sentence "... these arcs coincide with the most obliquely parts of contour lines while the outer contours are better overlapped than the inner ones" is confusing, and I find the subsequent discussion through page 6 difficult to follow.*

75 Reply:
This sentence and the following ones (Page 5, Line 16 to Page 6, Line 9 in the former manuscript) have been deleted. Instead, we introduced a new comment discussed above (Page 6, Line 6 to Line 11). The next paragraph in the former manuscript (Page 6, Line 10 to Line 14) was replaced by the following comment.

80 Changes in the manuscript:

– Page 6: Line 15 to Line 29:

"These results suggest that the damping of the ion sound waves excited by the field aligned parametric decay is the main mechanism of plasma heating in the 1D and 2D systems. In the 3D system, the protons are also heated in the perpendicular direction by the cyclotron damping of waves. The ions are perpendicular scattered by the field aligned and the oblique developed Alfvén daughter waves.

Figure 1 shows that the amplitude of the anti-parallel propagating Alfvén daughter wave decreases with increasing spatial dimension, while the level of the density fluctuation is similar. The power spectrum $\delta B^2(k_\parallel)$ is obtained by the Fourier transformation of the averaged magnetic field, $\delta\tilde{B}(r_\parallel) = \int \delta B(r_{\perp 1}, r_{\perp 2}, r_\parallel)dr_{\perp 1}dr_{\perp 2}$, in the assumption of strictly parallel wave propagation. Any deviation from the parallel direction will conduct to a reduction of the E^D amplitude of the daughter mode. A slight obliquity (several degrees) of the daughter wave mode is noticed in the 3D system but the reason remains unclear within the simulation work here and needs further investigations. The pitch-angle scattering and the perpendicular temperature increase observed in the time evolutions of the velocity distribution functions and temperatures, respectively, suggest that the Alfvén daughter waves are in cyclotron resonance with protons and the wave-particle interaction could explain the deviation in the propagation angle and the stronger damping of the daughter waves in the 3D system. A detailed spectral analyzing of the oblique wave modes developed in the decay process based on the 2D reduced magnetic field spectrum will be subject for a further study."

– *Add the t=0 contours to Figure 3, and compute the $T_\parallel$ and $T_\perp$ values as functions of time to quantify the statements in the discussion.*

Reply:
Done.

Changes in the manuscript:

– Fig. 3 is updated with time t=0.
– New Fig. 4 shows the time evolution of temperatures.

– *A central point of this manuscript is that the 3D simulations yield better results than the corresponding 1D and 2D results. This point should be made in the Abstract and repeated in the Conclusion section.*

Reply:
We thank the referee for this suggestion.

Changes in the manuscript:

– Abstract, Page 1: Line 3 to Line 6:
"The comparison made among different spatial dimensions proves that the three-dimensional

3

simulation exhibits more efficient heating. Plasma is heated parallel to the mean magnetic field by the damping of the ion acoustic waves while being heated perpendicular by the cyclotron resonance and damping of protons by Alfvén daughter waves."

– Conclusion, Page 6: Line 33 to Page 7 Line 4:
   "By comparing the wave modes and proton velocity distribution functions in 1D, 2D, and 3D systems, we conclude that the plasma is heated more efficient in the 3D system, thus proving that the 3D simulations yield better results than the corresponding 1D and 2D results. Parallel heating of plasma is provided by the damping of ion sound waves while perpendicular heating is given by the perpendicular scattering of protons by the field aligned and the oblique developed Alfvén daughter waves."

– *The proton velocity distributions measured from spacecraft in the fast solar wind often show a beam component and a core component with different relative densities and relative flow velocities parallel to the background magnetic field. Figure 3 of this manuscript shows two proton components of equal densities with relative flow velocities perpendicular to B_0. The Abstract claims the results of the simulations are in agreement with in situ measurements; to justify this claim, the authors need to explain these differences.*

Reply:
We reformulated the sentence as follows: "In the solar wind context, the antisunward part of the core component of the proton velocity distributions is controlled by the sunward-propagating waves driven by the parametric decay."

Changes in the manuscript:

– Page 1: Line 6 to Line 7
   "In the solar wind context, the antisunward part of the core component of the proton velocity distributions is controlled by the sunward-propagating waves driven by the parametric decay."

– *Title: There is no discussion or demonstration of wave breaking here, this word should be deleted from the title.*

Changes in the manuscript:

– Title: We replaced "breaking" by "parametric decay".

– *Page 2, Line 9: Delete so.*

Reply:
Done.

Changes in the manuscript:

4

– Page 2: Line 9.

– *Page 2, Line 23: Low-beta?*

Reply:
Done.

Changes in the manuscript:

  – Page: 2, Line 23: "low-beta plasmas."

– *Page 2, Line 31: in directions perpendicular ...*

Reply:
Done.

Changes in the manuscript:

  – Page: 2, Line: 31.
    "... in directions perpendicular to the mean magnetic field."

– *Page 3, Line 12: Replace circularly with circular.*

Reply:
Done.

Changes in the manuscript:

  – Page 3, Line 16.

– *Page 3, Line 15: Replace transversal with fluctuating.*

Reply:
Done.

Changes in the manuscript:

  – Page 3: Line 19
    "The initial fluctuating magnetic field ..."

- *Page 3, Lines 18-19: "The parametric decay modeled here is a 3-wave process involving a large-amplitude monochromatic Alfven pump wave propagating parallel to B_0, a spectrum of electrostatic ion acoustic waves also at parallel propagation, and a spectrum of Alfven daughter waves at anti-parallel propagation."*

Reply:
Done.

Changes in the manuscript:

- Page 3: Line 23 - 25
"The parametric decay modeled here is a three-wave process involving a large-amplitude monochromatic Alfvén pump wave propagating parallel to B_0, a spectrum of electrostatic ion acoustic waves also at parallel propagation, and a spectrum of Alfven daughter waves at anti-parallel propagation."

- *Page 3, Line 22: Delete linear (saturation is a nonlinear process).*
Reply:
Done.

Changes in the manuscript:

- Page 3: Line 28.

- *Page 3, Line 23: Delete nonlinear; it is unnecessary.*

Reply:
Done.

Changes in the manuscript:

- Page 3: Line 29.

- *Page 3, Line 33: ... and the lower panels correspond to the end of the simulation (t Ω_{cp} =600)."*

Reply:
Done.

Changes in the manuscript:

215   – Page 4: Line 7
"... and the lower panels correspond to the end of the simulation (t Ω_p =600)."

– *Page 6: Insert the definitions of the solid lines and the dashed lines in the caption to Figure 3.*

Reply:
Done.

220   Changes in the manuscript:

– Caption of Fig. 3:
"... The dashed lines describe the locus $(v_\parallel, v_\perp)$ of the particle velocities

$v = \sqrt{(v_\parallel - V_{ph})^2 + v_\perp^2}$ where their energy is conserved in the wave frame. Here V_{ph} is

225   the phase speed of the Alfvén wave."

Other changes in the manuscript:

– Page: 3, Line 11 to line 15
"The value of beta parameter 0.01 is set in order to keep the same value of beta in all the
230   1-D, 2-D, and 3-D setups for the purpose of comparison, and moreover, a lower value of
beta (such as 0.01) is not irrelevant from the solar wind studies. In fact, the solar wind
plasma originates in the corona and the low-beta plasmas are more representative in the
inner heliosphere. Therefore, we regard our numerical studies not only for understanding
the solar wind but also for understanding the solar corona."

235   – Page 4: Line 4 to Line 6
"The time evolution of the velocity distribution functions is usually helpful to emphasize
the role of the kinetic regime on the saturation of the instability via particle trapping and
wave particle interactions."

– Page 4: Line 13 to Line 16
240   "This is a consequence of the low values for the electron beta (β=0.01) and ion beta
(β=0.01) used in the simulation. At very low electron temperatures, the contribution of
the electron pressure term to the electric field ($\nabla P_e = \nabla n k_B T_e$) is small and the particle
density fluctuations n are less efficient in coupling to the electric field fluctuations."

On heating of solar wind protons by the ~~breaking~~ *parametric decay of large amplitude Alfvén waves*

Horia Comişel[1,2], Yasuhiro Nariyuki[3], Yasuhito Narita[4,5], and Uwe Motschmann[1,6]

[1]Institut für Theoretische Physik, Technische Universität Braunschweig, Mendelssohnstr. 3, D-38106 Braunschweig, Germany
[2]Institute for Space Sciences, Atomiştilor 409, P.O. Box MG-23, Bucharest-Măgurele, RO-077125, Romania
[3]Faculty of Human Development, University of Toyama, 3190, Gofuku, Toyama City, Toyama 930-8555, Japan
[4]Space Research Institute, Austrian Academy of Sciences, Schmiedlstr. 6, A-8042 Graz, Austria
[5]Institut für Geophysik und extraterrestrische Physik, Technische Universität Braunschweig, Mendelssohnstr. 3, D-38106 Braunschweig, Germany
[6]Deutsches Zentrum für Luft- und Raumfahrt, Institut für Planetenforschung, Rutherfordstr. 2, D-12489 Berlin, Germany

Correspondence: H. Comişel
(h.comisel@tu-braunschweig.de)

Abstract.

By means of hybrid simulations, we present a study on ~~plasma~~ **ion** heating by the field-aligned parametric decay of a monochromatic left-hand polarized Alfvén wave. **The comparison made among different spatial dimensions proves that the three-dimensional simulation exhibits more efficient heating. Plasma is heated parallel to the mean magnetic field by the damping of the ion acoustic waves while being heated perpendicular by the cyclotron resonance and damping of protons by Alfvén daughter waves. In the solar wind context, the antisunward part of the core component of the proton velocity distributions is controlled by the sunward-propagating waves driven by the parametric decay.**

Keywords. Space plasma physics (Wave-wave interactions, Wave-particle interactions, Numerical simulation studies).

1 Introduction

Early in situ measurements at 1AU from VELA satellite (Bame et al., 1975) reveal that the velocity distribution function of solar wind protons is broader in direction perpendicular to the mean magnetic field compared to the parallel distribution, thus indicating that the perpendicular temperature is higher than the parallel temperature. Marsch et al. (1982) have found by using Helios 1 and Helios 2 data such plasma heating occurring in high speed solar wind streams from 0.3 to 1.0 AU. The problem of acceleration and heating of ions in solar wind and solar corona is vast and has been discussed for a long time in space plasma physics, see e.g., the reviews of Marsch (2006); Ofman (2010). Theoretical models based on cyclotron resonant- or non-resonant- processes have been proposed to explain the heating of solar corona and solar wind. All of these models are related to the pitch angle scattering of protons.

Marsch and Tu (2001) have shown for the first time the observational evidence for the occurrence of the pitch angle scattering of solar wind protons, driven by resonance with ion cyclotron waves propagating outwards the Sun. The ions in resonance with transversal cyclotron waves conserve their total kinetic energy in a frame moving with the phase velocity of the wave while their velocity distribution functions show a plateau observed through circular contours of constant density in phase space. Thus, the perpendicular broadening of the left hand part of the measured distributions (the sunward part) has been explained through the pitch angle scattering of solar wind protons resonantly interacting with the outward propagating waves. However, this process cannot explain the antisunward part of the core distribution. Araneda et al. (2007) suggest, on basis of the conclusions discussed by Marsch and Tu (2001), that a candidate which is able to elucidate this mystery could be the parametric decay instability, a process so rarely detected by in situ measurements in space plasmas (see e.g., Spangler et al., 1997).

Parametric instabilities play an important role in the dissipation of the large amplitude Alfvén waves with parallel or quasi-parallel propagation with respect to the mean magnetic field and in plasma heating by means of the ion Landau damping mechanism. Parametric instabilities including decay, modulational, and beat instabilities, have been extensively analyzed by theoretical studies (see e.g., Viñas and Goldstein , 1991) or numerical magnetohydrodynamics MHD (e.g., Ghosh et al., 1993; Ghosh and Goldstein, 1994; Del Zanna et al., 2001) and particle-in-cell or hybrid (e.g., Terasawa et al., 1986; Matteini et al., 2010a, b; Verscharen et al., 2012; Gao et al., 2013; Nariyuki et al., 2014) simulations. In the MHD picture, the plasma heating by the Alfvén wave can occur through generation and steepening of magnetosonic waves. A shock wave is formed as a result of the wave steepening at a late (and nonlinear) saturation stage of the parametric decay. In the kinetic picture, hybrid simulations prove that the heating mechanism is completed by kinetic effects and a beam can be created in the ion distribution function due to the non-linear trapping of protons (see e.g., Araneda et al., 2008; Matteini et al., 2010a, b). By using hybrid simulations, Nariyuki et al. (2012) show that monochromatic Alfvén waves with circular left-handed polarization are quickly dissipated by a beam driven by kinetic Alfvén waves. Nariyuki et al. (2014) also discuss on the collisionless damping of the field aligned Alfvén waves at low frequency in solar wind plasmas with or without the presence of a proton beam. The velocity beam formation is however restricted by the conditions of **low-**beta plasmas. On the assumption of cold electrons, the electric field is decoupled from the density fluctuations and the formation of the beam is inhibited (see e.g., Matteini et al., 2010a). By means of 2D hybrid simulations, Gao et al. (2013) recently suggest that under such conditions relevant for the solar corona, the obliquely-propagating Alfvén daughter waves driven by the parametric decay could stochastically heat the plasma.

Here we present a numerical study on plasma heating by the decay of a large amplitude monochromatic Alfvén wave propagating along the mean magnetic field in a multidimensional simulation box immersed in a uniform low beta electron proton collisionless plasma. By analyzing the velocity distribution functions and the time history of the wave modes obtained from one-, two-, and three- dimensional hybrid simulations, we report that parametric decay and pitch angle scattering mechanisms are both involved in broadening the entire proton velocity distribution in directions perpendicular to the mean magnetic field. The left-handed circularly polarized Alfvén pump wave with forward propagation does perpendicularly broaden one side of the particle velocity distributions while the backward propagating Alfvén daughter wave enlarges the other side, respectively.

2 Hybrid simulation and discussion on results

The hybrid simulations are conducted in 1D, 2D and 3D setups by using the hybrid code AIKEF (Müller et al., 2011). The one-dimensional box has a length of L_1=720 d_i while in the two-dimensional setup, L_1=L_2=288 d_i on each direction. Here, $d_i = V_A/\Omega_p$ is the ion inertial length while V_A and Ω_p are the Alfvén velocity and the ion gyrofrequency, respectively. A number of N_c=10000 super-particles is introduced in each computational cell. By adding the third dimension (L_3=288 d_i), the number of super-particles is diminished to N_c=1000 particles in a cell. Even so, the total number of super-particles used in the 3D system ($N_t \approx 2.0 \cdot 10^{10}$) is at the limit of our computational resources but it is sufficient to reduce the influence of numerical noise in agreement with additional 3D tests carried out by using smaller sizes of the box (L_1=L_2=L_3=144 d_i), and a larger number of super-particles in the simulation cell (N_c=2500). The grid size is the same for all the cases and equals the ion inertial length (d_i). A low value of β=0.01 is used for the plasma beta parameter for each species of particles, namely the protons treated in the hybrid scheme as particles and the electrons considered as a massless fluid. **The value of beta parameter 0.01 is set in order to keep the same value of beta in all the 1-D, 2-D, and 3-D setups for the purpose of comparison, and moreover, a lower value of beta (such as 0.01) is not irrelevant from the solar wind studies. In fact, the solar wind plasma originates in the corona and the low-beta plasmas are more representative in the inner heliosphere. Therefore, we regard our numerical studies not only for understanding the solar wind but also for understanding the solar corona.** At the initial time, a monochromatic Alfvén pump wave with left-handed ~~circular~~ly polarization is launched parallel to the mean magnetic field along the Oz axis of the simulation box. The amplitude of the pump wave is set to 20% of the mean magnetic field magnitude, $\delta B/B_0$=0.2. The wavenumber of the pump wave is $k_0 V_A/\Omega_p = 0.218$, corresponding to a Fourier mode of m=10 (m=25 for the 1D system). The initial ~~transversal~~ **fluctuating** magnetic field ($\boldsymbol{B}_\perp$) and bulk velocity ($\boldsymbol{u}_\perp$) satisfies the relation $\boldsymbol{u}_\perp = -k_0/\omega_0 \boldsymbol{B}_\perp$, while the resonant frequency ω_0=0.196 Ω_p, is determined from the dispersion relation $k_0^2 = \omega_0^2/(1 - \omega_0)$ for the left-handed waves, (see e.g., Terasawa et al., 1986). The initial setup of the pump waves is identical for all the 1D, 2D and 3D configurations.

The parametric decay modeled here is a three-wave process involving a large-amplitude monochromatic Alfvén pump wave propagating parallel to B_0, a spectrum of electrostatic ion acoustic waves also at parallel propagation, and a spectrum of Alfvén daughter waves at anti-parallel propagation. Figure 1 shows the time profiles for the magnetic field energy of the pump wave (labeled by E^P) and the backward propagating Alfvén daughter waves (labeled by E^D) for the 2D setup (left panel) and the 3D setup (right panel). Overplotted by gray solid lines are the root mean square (rms) density fluctuations (ρ) with a maximum at about 300 ion gyroperiods when the linear growing of E^D terminates, i.e., the ~~linear~~ saturation of the instability occurs. At the ~~nonlinear~~ saturation time when the energy of the daughter wave overtakes the energy of the mother wave, the frequency-wavenumber power spectrum of the magnetic field is shown in the lower panels of Fig. 1. The left-handed pump wave (here we adopted the convention of negative frequency for the left-handed mode) marked with E^P can be seen in the lower-right quadrant ($k > 0$ and $\omega < 0$) while the counter-propagating Alfvén daughter wave (E^D) is developed in the lower-left quadrant ($k < 0$ and $\omega < 0$) of the frequency-wavenumber spectrum and has the Fourier mode m=-8 (m=-23 for the 1D run, not shown here). The waves driven by the decay instability dominate the entire spectrum.
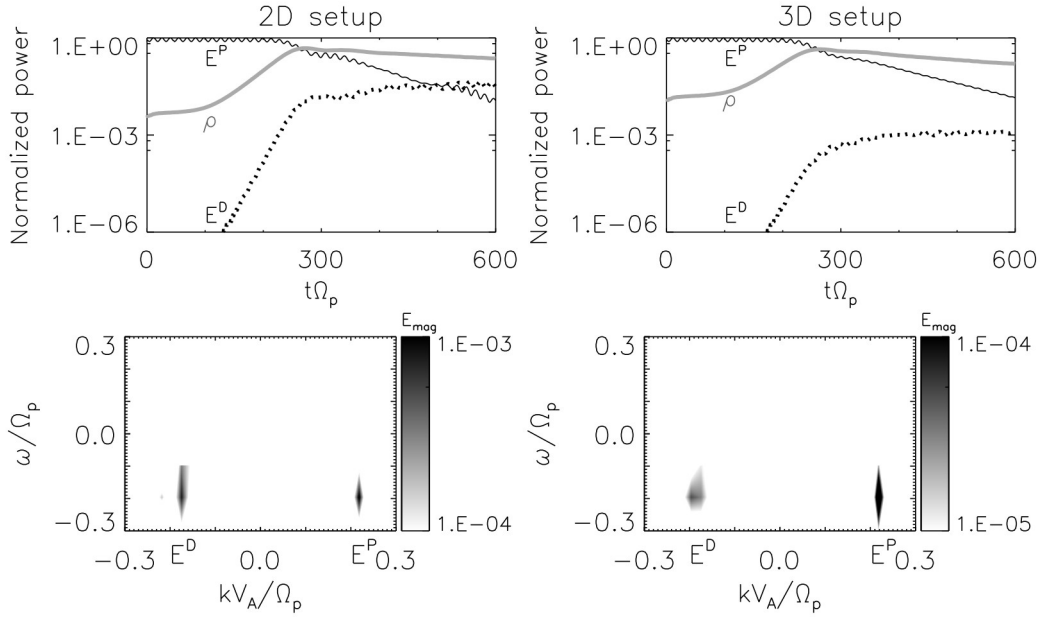
Figure 1. Top: Time evolution of the normalized magnetic field energy of the Alfvén pump wave (E^P) and the counter propagating Alfvén daughter wave (E^D). Overplotted by gray are given the rms density fluctuations ρ. Bottom: Power spectrum in the wavenumber frequency domain of the magnetic field determined around time $t\Omega_p \sim 500$.

Qualitatively speaking, the results presented in Fig. 1 are consistent with the earlier MHD studies, proving that the parametric decay responsible for the breaking of the Alfvén pump wave occurs irrespective of the spatial dimensions.

Figure 2 shows the particle distribution functions in the phase space $z - v_\parallel$ at two different stages for the evolution of decay instability in the 2-D and 3-D setup. **The time evolution of the velocity distribution functions is usually helpful to**
5   **emphasize the role of the kinetic regime on the saturation of the instability via particle trapping and wave particle interactions.** The upper panels of Fig. 2 refer to the linear stage of the instability at a time of $t\Omega_p \sim 300$ and the lower panels **correspond to the end of the simulation** ($t\Omega_p = 600$). The number of particles is represented in a color code scale with a minimum defined by the lightest nuance of gray. At the linear stage, the protons are accelerated by the parallel electric field produced by the density fluctuations. The proton phase space $z - v_\parallel$ is close to the result from an earlier study. Matteini et
10   al. (2010a) explain the spatial modulation and the modulation in enhancement of the parallel electric field (Fig. 5 in their paper) due to the broader spectrum of ion acoustic waves excited by the large amplitude Alfvén mother wave. The spatial modulation in Fig. 2 is weaker according to the smaller amplitude pump wave used in our simulation. During the saturation of the instability we do not observe the presence of phase-space vortices leading to the formation of a proton beam. **This is a consequence of the low values for the electron beta (β=0.01) and ion beta (β=0.01) used in the simulation. At very low**
15   **electron temperatures, the contribution of the electron pressure term to the electric field ($\nabla P_e = \nabla n k_B T_e$) is small and the particle density fluctuations n are less efficient in coupling to the electric field fluctuations.** The proton phase space at
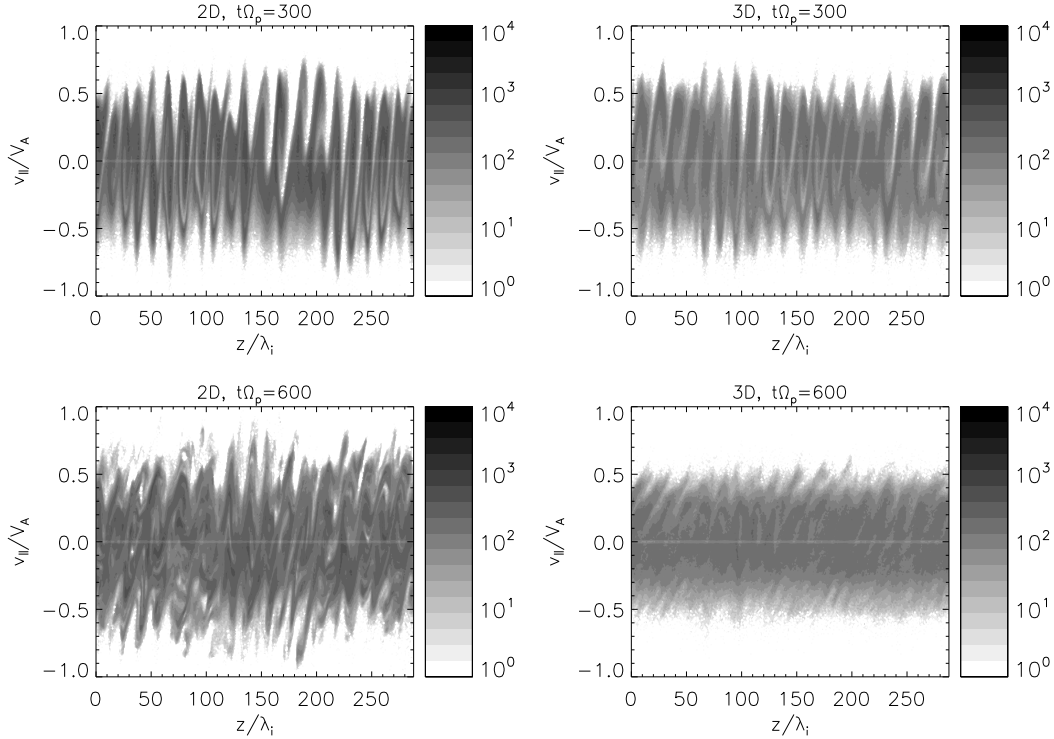
Figure 2. Top: Proton phase space $z - v_\parallel$ at time $t\Omega_p = 300$ close to the linear saturation of the decay instability. Bottom: Proton phase space $z - v_\parallel$ at the final time $t\Omega_p = 600$ of the simulation.

the linear stage of the instability does not differ too much between the 2D and 3D runs. The velocity distribution, in contrast, is different for the 3D system at the nonlinear stage of the instability as one can see in the lower panels of Fig. 2. Particles are smoothly heated and the resonant protons accelerated by the ion acoustic waves are mixed with the thermal core of the distribution.

5   Figure 3 reports a comparison of the proton velocity distribution functions constructed in the $(v_\perp, v_\parallel)$ plane obtained from the one-, two-, and three- dimensional systems **at the initial time** and at the same simulation epochs as in Figure 2. **The velocity distribution function f is computed by counting the number of particles $dN = f(v_\perp, v_\parallel, \Phi)dV$ in the volume element $dV = v_\perp dv_\perp dv_\parallel d\Phi$, and by integrating over the azimuthal Φ angle. Here, $v_\perp = \sqrt{v_{\perp 1}^2 + v_{\perp 2}^2}$ is the velocity component perpendicular to the mean magnetic field, $v_\parallel$ is the parallel velocity, and the angle $\Phi = \arctan v_{\perp 1}/v_{\perp 2}$ gives the sign of**

10 $v_\perp$**.** The contour lines are shown for fractions of 0.6, 0.3, 0.2, and 0.1 of the maximum phase space density from the inner to the outer part of the distribution functions. **Due to the transversal wave field imposed at the initial condition, the velocity distribution functions are rigid shifted towards the initial bulk velocity $\pm u_\perp$, see e.g., Verscharen and Marsch (2011); Nariyuki (2011). The two symmetrical sets of contour levels with respect to the $v_\perp = 0$ axis are slowly merging with the time evolution and at time $t\Omega_p$=300 there are no remnants of the rigid displacement observed at the initial time.** Similar

with Fig. 2, the velocity distribution functions ~~obtained from the 2D and 3D setups~~ do not clearly differ close to the linear stage of the decay instability at time $t\Omega_{\mathrm{p}}$=300. The dashed lines represent arcs of circles with centers localized along the $v_{\parallel}$ axis at the position corresponding to the phase velocities of Alfvén pump wave ($V_{ph} = \omega_0/k_0 V_{\mathrm{A}} \approx$-0.9) and Alfvén daughter wave ($V_{ph} = \omega/k V_{\mathrm{A}} \approx$+0.9), respectively. They describe the particle velocity in the wave frame, $v = \sqrt{(v_{\parallel} - V_{ph})^2 + v_{\perp}^2}$.

5 According to pitch angle scattering model, the particle energy, E=mv^2/2, is conserved in this reference system.

Although there are no obvious differences in the three analyzed setups, one can notice a distinct trend of evolution for the distributions between the intermediate ($t\Omega_p$=300) and the final time of simulation ($t\Omega_p$=600). At the final time, the contour levels in the 3D simulation are moderately enlarging both in the parallel and perpendicular directions by following the contour levels of energy conservation driven by the pitch-angle scattering of protons. The contour levels in

10 **1D and 2D runs, in contrast, are developing mainly towards parallel direction while their initial perpendicular displacement is removing with time elapsing. The more efficient heating of plasma in the 3D system is consistent with the time evolution of the ion temperature shown in Figure 4. The particles experience a similar parallel heating while the perpendicular temperature achieved in the 3D system (solid line) dominates by a factor of two or more the corresponding values obtained in the 1D (dotted line) and 2D (dashed line) simulations.**

15 **These results suggest that the damping of the ion sound waves excited by the field aligned parametric decay is the main mechanism of plasma heating in the 1D and 2D systems. In the 3D system, the protons are also heated in the perpendicular direction by the cyclotron damping of waves. The ions are perpendicular scattered by the field aligned and the oblique developed Alfvén daughter waves.**

Figure 1 shows that the amplitude of the anti-parallel propagating Alfvén daughter wave decreases with increasing

20 **spatial dimension, while the level of the density fluctuation is similar. The power spectrum $\delta B^2(k_{\parallel})$ is obtained by the Fourier transformation of the averaged magnetic field, $\delta \tilde{B}(r_{\parallel}) = \int \delta B(r_{\perp 1}, r_{\perp 2}, r_{\parallel}) dr_{\perp 1} dr_{\perp 2}$, in the assumption of strictly parallel wave propagation. Any deviation from the parallel direction will conduct to a reduction of the E^D amplitude of the daughter mode. A slight obliquity (several degrees) of the daughter wave mode is noticed in the 3D system but the reason remains unclear within the simulation work here and needs further investigations. The pitch-angle**

25 **scattering and the perpendicular temperature increase observed in the time evolutions of the velocity distribution functions and temperatures, respectively, suggest that the Alfvén daughter waves are in cyclotron resonance with protons and the wave-particle interaction could explain the deviation in the propagation angle and the stronger damping of the daughter waves in the 3D system. A detailed spectral analyzing of the oblique wave modes developed in the decay process based on the 2D reduced magnetic field spectrum will be subject for a further study.**

30 ## 3   Conclusion

We studied the proton acceleration and heating driven by the parametric decay of a large amplitude Alfvén wave in the linear and nonlinear stage of the instability in a multidimensional system. By comparing the wave modes and proton velocity distribution functions **in 1D, 2D, and 3D systems, we conclude that the plasma is heated more efficient in the 3D system,**
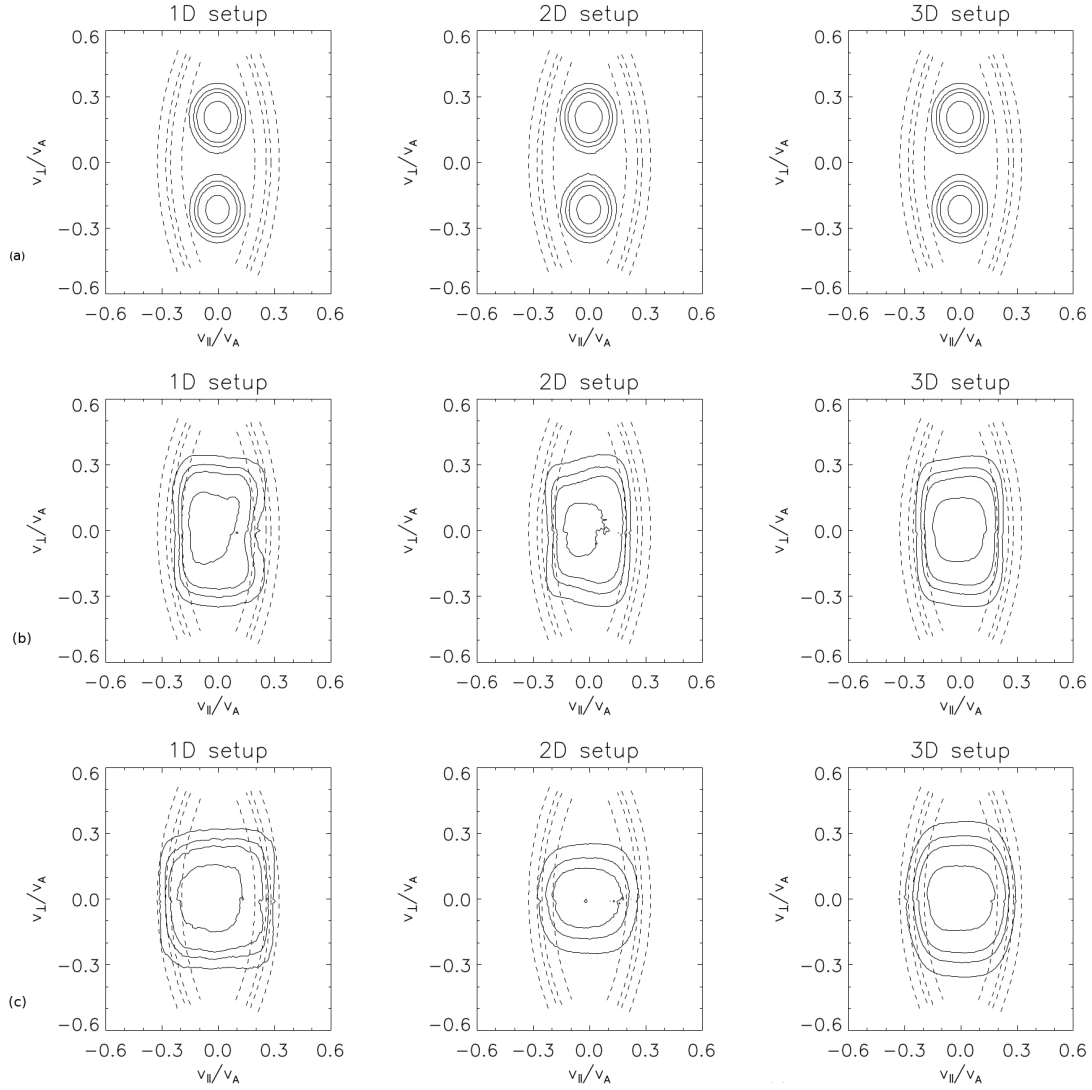
Figure 3. Proton distribution functions represented as contour levels (solid line) determined in the plane ($v_\perp$,$v_\parallel$) **at times** $t\Omega_p$**=0 (a),** $t\Omega_p$**=300** **(b), and** $t\Omega_p$**=600 (c). The dashed lines describe the locus** ($v_\parallel, v_\perp$) **of the particle velocities** $v = \sqrt{(v_\parallel - V_{ph})^2 + v_\perp^2}$ **where their energy is conserved in the wave frame. Here** V_{ph} **is the phase speed of the Alfvén wave.**

thus proving that the 3D simulations yield better results than the corresponding 1D and 2D results. Parallel heating of plasma is provided by the damping of ion sound waves while perpendicular heating is given by the perpendicular scattering of protons by the field aligned and the oblique developed Alfvén daughter waves. The pitch-angle scattering is the mechanism able to describe the perpendicular broadening observed in the particle velocity distribution functions.

5   In the 3D system, the conditions for resonant cyclotron interactions of ions with the left-handed Alfvén waves are apparently

7
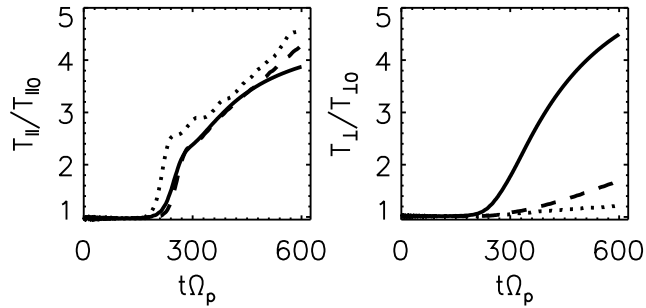
Figure 4. Time evolution of the parallel ($T_\parallel$) and perpendicular ($T_\perp$) proton temperatures for the 1-D (dotted line), 2-D (dashed line), and 3-D (solid line) configurations. The temperatures are normalized to their initial values.

fulfilled especially at the non-linear stage evolution of the decay process. Further studies are needed for a better understanding of this circumstance by using a larger panel of initial resonant conditions for the particles and wave fields, or different values of the ion and electron temperatures.

Tsurutani et al. (2005) discuss on a close relation between the perpendicular acceleration of protons, the phase-steepened
5 Alfvén waves, and the magnetic field decreases observed preponderantly in the fast streams of interplanetary solar wind. Parametric decay and pitch angle scattering could play also a role for a better understanding of the connection between the mentioned observations. Nevertheless, the result discussed in this paper can invoke that that parametric decay, besides its implication in the reduction of the cross-helicity in the solar wind and in the local production of turbulence, would also play a key role in pitch angle scattering of the solar wind protons and finally in the perpendicular temperature anisotropy observed in
10 the inner heliosphere.

References

Araneda, J. A., Marsch, and E., Viñas, A. F.: Collisionless damping of parametrically unstable Alfvén waves, J. Geophys. Res., 112, A04104, https://doi.org/10.1029/2006JA011999, 2007.

Araneda, J. A., Marsch, E., and Viñas, A. F.: Proton Core Heating and Beam Formation via Parametrically Unstable Alfvén-Cyclotron Wave, Phys. Rev. Lett., 100, 12, https://doi.org/10.1103/PhysRevLett.100.125003, 2008.

Bame, S. J., Asbridge, J. R., Feldman, W. C., Montgomery, M. D., Gary, S. P.: Evidence for local ion heating in solar wind high speed streams, Geophys. Res. Lett., 2, 373, https://doi.org/10.1029/GL002i009p00373, 1975.

Del Zanna, L., Velli, M., and Londrillo, P.: Parametric decay of circularly polarized Alfvén waves: Multidimensional simulations in periodic and open domains, Astron. Astrophys. 367, 705-718, https://doi.org/10.1051/0004-6361:20000455, 2001.

Gao, X., Lu, Q., Li, X., Shan, L., and Wang., S.: Parametric instability of a monochromatic Alfven wave: Perpendicular decay in low beta plasma, Phys. Plasmas 20, 072902, https://doi.org/10.1063/1.4816703, 2013.

Ghosh, S., Viñas, A. F., and Goldstein, M. L.: Parametric instabilities of a large-amplitude circularly polarized Alfvén wave: Linear growth in two-dimensional geometries, J. Geophys. Res., 98, 15561–15570, https://doi.org/10.1029/93JA01534, 1993.

Ghosh, S., Goldstein, M. L.: Nonlinear evolution of a large-amplitude circularly polarized Alfvén wave: Low beta, J. Geophys. Res., 99, 13351-13362, https://doi.org/10.1029/94JA00474, 1994.

Marsch, E., Mühlhäuser, K.-H., Schwenn, R., Rosenbauer, H., Pilipp, W., Neubauer, F. M.: Solar wind protons: Three-dimensional velocity distributions and derived plasma parameters measured between 0.3 and 1 AU, J. Geophys. Res., 87, 52, https://doi.org/10.1029/JA087iA01p00052, 1982.

Marsch, E. and Tu, C.-Y.: Evidence for pitch angle diffusion of solar wind protons in resonance with cyclotron waves, J. Geophys. Res., 106, 8357, https://doi.org/10.1029/2000JA000414, 2001.

Marsch, E.:Kinetic physics of the solar corona and solar wind, Living Rev. Solar Phys., 3, http://livingsreviews.org/lrsp-2006-1, 2006.

Matteini, L., Landi, S., Del Zanna, L., Velli, M., Hellinger, P.: Kinetics of parametric instabilities of Alfvén waves: Evolution of ion distribution functions, J. Geophys. Res., 115, A09106, https://doi.org/10.1029/2009JA014987, 2010a.

Matteini, L., Landi, S., Del Zanna, L., Velli, M., Hellinger, P.: Parametric decay of linearly polarized shear Alfvén waves in oblique propagation: One and two-dimensional hybrid simulations, Geophys. Res. Lett., 37, L20101, https://doi.org/10.1029/2010GL044806, 2010b.

Müller, J., Simon, S., Motschmann, U., Schüle, J., Glassmeier, K. -H. and Pringle, G. J.: A.I.K.E.F.: Adaptive hybrid model for space plasma simulations, Comp. Phys. Comm., 182, 946-966, https://doi.org/10.1016/j.cpc.2010.12.033, 2011.

Nariyuki, Y.: On entropy-maximized velocity distributions in circularly polarized finite amplitude Alfvén waves, Phys. Plasmas, 18, 052 112, 2011.

Nariyuki, Y., Hada, T., and Tsubouchi, K.: Nonlinear dissipation of circularly polarized Alfvén waves due to the beam-induced obliquely propagating waves, Phys. Plasmas 19, 082317, https://doi.org/10.1063/1.4748296, 2012.

Nariyuki, Y., Hada, T., and Tsubouchi, K.: Collisionless Damping of Circularly Polarized Nonlinear Alfvén Waves in Solar Wind Plasmas with and without Beam Protons, Astrophys. J., 793, 138, https://doi.org/10.1088/0004-637X/793/2/138, 2014.

Ofman, L.: Wave modeling of solar wind, Living Rev. Solar Phys., 7, https://doi.org/doi:10.12942/lrsp-2010-4, 2010.

Spangler, S. R., Leckband, J.A., and Cairns, I. H.: Observations of the parametric decay instability of nonlinear magnetohydrodynamic waves, Phys. Plasmas, 4, 846, https://doi.org/doi:10.1063/1.872183, 1997.

Terasawa, T., Hoshino, M., Sakai, J.-I., and Hada, T.: Decay instability of finite-amplitude circularly polarized Alfven Waves: A numerical simulation of stimulated Brillouin scattering, J. Geophys. Res., 91, 4171-4187, https://doi.org/10.1029/JA091iA04p04171, 1986.

Tsurutani, B., G. S. Lakhina, G. S., Pickett, J. S., Guarnieri, F. L., Lin, N., and Goldstein, B. E.: Nonlinear Alfvén waves, discontinuities, proton perpendicular acceleration, and magnetic holes/decreases in interplanetary space and the magnetosphere: intermediate shocks?, Nonlin. Processes Geophys., 12, 321, https://doi.org/10.5194/npg-12-321-2005, 2005.

Verscharen, D. and Marsch, E.: Apparent temperature anisotropies due to wave activity in the solar wind, Ann. Geophys., 29, 909, https://doi.org/10.5194/angeo-29-909-2011.

Verscharen, D., Marsch, E., Motschmann, U., and Müller, J.: Parametric decay of oblique Alfvén waves in two-dimensional hybrid simulations, Phys. Rev. E, 86, 027401, https://doi.org/10.1103/PhysRevE.86.027401, 2012.

Viñas, A. F. and Goldstein M. L.: Parametric instabilities of circularly polarized large-amplitude dispersive Alfvén waves: excitation of obliquely-propagating daughter and side-band waves, J. Plasma Phys., 46, 129, https://doi.org/10.1017/S0022377800015993, 1991.